

Real-valued (Medical) Time Series Generation with Recurrent Conditional GANs

Stephanie L. Hyland^{*1, 2}, Cristóbal Esteban^{*1}, Gunnar Rätsch¹

¹Department of Computer Science, ETH Zurich, Switzerland

²Tri-Institutional Training Program in Computational Biology and Medicine, Weill Cornell Medical
 {stephanie.hyland, cristobal.esteban, raetsch}@inf.ethz.ch

*Authors contributed equally.

Abstract

Generative Adversarial Networks (GANs) have shown remarkable success as a framework for training models to produce realistic-looking data. In this work, we propose a Recurrent GAN (RGAN) and Recurrent Conditional GAN (RCGAN) to produce realistic *real-valued multi-dimensional time series*, with an emphasis on their application to medical data. RGANs make use of recurrent neural networks in the generator and the discriminator. In the case of RCGANs, both of these RNNs are conditioned on auxiliary information. We demonstrate our models in a set of toy datasets, where we show visually and quantitatively (using sample likelihood and maximum mean discrepancy) that they can successfully generate realistic time-series. We also describe novel evaluation methods for GANs, where we generate a synthetic labelled training dataset, and evaluate on a *real test set* the performance of a model trained on the *synthetic data*, and vice-versa. We illustrate with these metrics that RCGANs can generate time-series data useful for supervised training, with only minor degradation in performance on *real* test data. This is demonstrated on digit classification from ‘serialised’ MNIST and by training an early warning system on a medical dataset of 17,000 patients from an intensive care unit. We further discuss and analyse the privacy concerns that may arise when using RCGANs to generate realistic synthetic medical time series data.

1 Introduction

Access to data is one of the bottlenecks in the development of machine learning solutions to domain-specific problems. The availability of standard datasets (with associated tasks) has helped to advance the capabilities of learning systems in multiple tasks. However, progress appears to lag in other fields, such as medicine. It is tempting to suggest that tasks in medicine are simply harder - the data more complex, more noisy, the prediction problems less clearly defined. Regardless of this, the dearth of data *accessible* to researchers hinders model comparisons, reproducibility and ultimately scientific progress. However, due to the highly sensitive nature of medical data, its access is typically highly controlled, or require involved and likely imperfect de-identification. The motivation for this work is therefore to exploit and develop the framework of generative adversarial networks (GANs) to generate realistic *synthetic* medical data. This data could be shared and published without privacy concerns, or even used to augment or enrich similar datasets collected in different or smaller cohorts of patients. Moreover, building a system capable of synthesizing realistic medical data implies modelling the processes that generates such information, and therefore it can represent the first step towards developing a new approach for creating predictive systems in medical environments.

Beyond the utility to the machine learning research community, such a tool stands to benefit the medical community for use in training simulators. In this work, we focus on synthesising real-valued time-series data as from an Intensive Care Unit (ICU). In ICUs, doctors have to make snap decisions under time pressure, where they cannot afford to hesitate. It is already standard in medical training to use simulations to train doctors, but these simulations often rely on hand-engineered rules and physical props. Thus, a model capable of generating diverse and realistic ICU situations could have an immediate application, especially when given the ability to condition on underlying ‘states’ of the patient.

The success of GANs in generating realistic-looking images [21, 15, 8, 22] suggests their applicability for this task, however limited work has exploited them for generating *time-series* data. In addition,

evaluation of GANs remains a largely-unsolved problem, with researchers often relying on visual evaluation of generated examples, an approach which is both impractical and inappropriate for multi-dimensional medical time series.

The primary contributions of this work are:

1. Demonstration of a method to generate real-valued sequences using adversarial training.
2. Showing novel approaches for evaluating GANs.
3. Generating synthetic medical time series data.

2 Related Work

Since their inception in 2014 [9], the GAN framework has attracted significant attention from the research community, and much of this work has focused on image generation [21, 15, 8, 22]. Notably, [7] designed a GAN to generate synthetic electronic health record (EHR) datasets. These EHRs contain binary and count variables, such as ICD-9 billing codes, medication, and procedure codes. Their focus on discrete-valued data and generating snapshots of a patient is complementary to our real-valued, time series focus. Future work could combine these approaches to generate multi-modal synthetic medical time-series data.

The majority of sequential data generation with GANs has focused on discrete tokens useful for natural language processing [28], where an alternative approach based on Reinforcement Learning (RL) is used to train the GAN. We are aware of only one preliminary work using GANs to generate *continuous-valued* sequences, which aims to produce polyphonic music using a GAN with LSTM generator and discriminator [19]. The primary differences are architectural: we do not use a bidirectional discriminator, and outputs of the generator are not fed back as inputs at the next time step. Moreover, we introduce also a conditional version of this Recurrent GAN.

Conditional GANs [18, 8] condition the model on additional information and therefore allow us to direct the data generation process. This approach has been mainly used for image generation tasks [21, 18, 2]. Recently, Conditional GAN architectures have been also used in natural language processing, including translation [27] and dialogue generation [16], where none of them uses an RNN as the preferred choice for the discriminator and, as previously mentioned, a RL approach is used to train the models due to the discrete nature of the data.

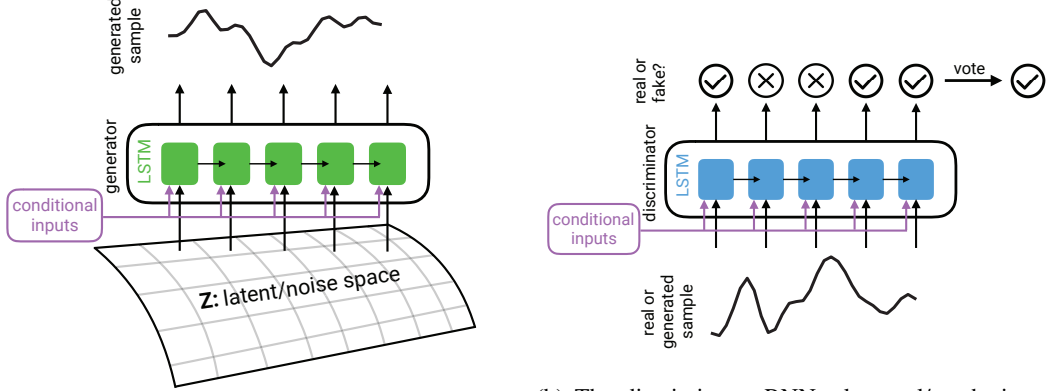
In this work, we also introduce some novel approaches to evaluate GANs, using the capability of the generated synthetic data to train supervised models. In a related fashion, a GAN-based semi-supervised learning approach was introduced in [23]. However, our goal is to generate data that can be used to train models for tasks that are unknown at the moment the GAN is trained.

3 Models: Recurrent GAN and Recurrent Conditional GAN

The model presented in this work follows the architecture of a regular GAN, where both the generator and the discriminator have been substituted by recurrent neural networks. Therefore, we present a Recurrent GAN (RGAN), which can generate sequences of real-valued data, and a Recurrent Conditional GAN (RCGAN), which can generate sequences of real-value data subject to some conditional inputs. As depicted in Figure 1a, the generator RNN takes a different random seed at each time step, plus an additional input if we want to condition the generated sequence with additional data. In Figure 1b, we show how the discriminator RNN takes the generated sequence, together with an additional input if it is a RCGAN, and produces a classification as synthetic or real for each time step of the input sequence.

Specifically, the discriminator is trained to minimise the average negative cross-entropy between its predictions *per time-step* and the labels of the sequence. If we denote by $\text{RNN}(X)$ the vector or matrix comprising the T outputs from a RNN receiving a sequence of T vectors $\{\mathbf{x}_t\}_{t=1}^T$ ($\mathbf{x}_t \in \mathbb{R}^d$), and by $\text{CE}(\mathbf{a}, \mathbf{b})$ the *average* cross-entropy between sequences \mathbf{a} and \mathbf{b} , then the discriminator loss for a pair $\{X_n, \mathbf{y}_n\}$ (with $X_n \in \mathbb{R}^{T \times d}$ and $\mathbf{y}_n \in \{1, 0\}^T$) is:

$$\text{D}_{\text{loss}}(X_n, \mathbf{y}_n) = -\text{CE}(\text{RNN}_D(X_n), \mathbf{y}_n)$$



(a) The generator RNN takes a different random seed at each temporal input, and produces a synthetic signal. In the case of the RCGAN, it also takes an additional input on each time step that conditions the output.

(b) The discriminator RNN takes real/synthetic sequences and produces a classification into real/synthetic for each time step. In the case of the RCGAN, it also takes an additional input on each time step that conditions the output.

Figure 1: Architecture of Recurrent GAN and Conditional Recurrent GAN models.

For real sequences, \mathbf{y}_n is a vector of 1s, or 0s for synthetic sequences. In each training minibatch, the discriminator sees both real and synthetic sequences.

The objective for the generator is then to ‘trick’ the discriminator into classifying its outputs as true, that is, it wishes to minimise the (average) negative cross-entropy between the discriminator’s predictions on *generated* sequences and the ‘true’ label, the vector of 1s (we write as $\mathbf{1}$);

$$G_{\text{loss}}(Z_n) = D_{\text{loss}}(\text{RNN}_G(Z_n), \mathbf{1}) = -\text{CE}(\text{RNN}_D(\text{RNN}_G(Z_n)), \mathbf{1})$$

Here Z_n is a sequence of T points $\{\mathbf{z}_t\}_{t=1}^T$ sampled *independently* from the latent/noise space \mathbf{Z} , thus $Z_n \in \mathbb{R}^{T \times m}$ since $\mathbf{Z} = \mathbb{R}^m$. Initial experimentation with non-independent sampling did not indicate any obvious benefit, but would be a topic for further investigation.

In this work, the architecture selected for both discriminator and generator RNNs is the LSTM [12].

In the conditional case (RCGAN), the inputs to each RNN are augmented with some conditional information \mathbf{c}_n (for sample n , say) by concatenation at *each* time-step;

$$\mathbf{z}_{nt} \rightarrow [\mathbf{z}_{nt}; \mathbf{c}_n] \quad \mathbf{x}_{nt} \rightarrow [\mathbf{x}_{nt}; \mathbf{c}_n]$$

In this way the RNN cannot discount the conditional information through forgetting.

Promising research into alternative GAN objectives, such as the Wasserstein GAN [3, 11] unfortunately do not find easy application to RGANs in our experiments. Enforcing the Lipschitz constraint on an RNN is a topic for further research, but may be aided by use of unitary RNNs [4, 13].

All models and experiments were implemented in python with scikit-learn [20] and Tensorflow [1], and the code is available here: <https://github.com/ratschlab/RGAN>.

3.1 Evaluation

Evaluating the performance of a GAN is challenging. As illustrated in [25] and [26], evaluating likelihoods, with Parzen window estimates [26] or otherwise can be deceptive, and the generator and discriminator losses do not readily correspond to ‘visual quality’. This nebulous notion of quality is best assessed by a human judge, but it is impractical and costly to do so. In the imaging domain, scores such as the Inception score [23] have been developed to aid in evaluation, and Mechanical Turk exploited to distribute the human labour. However, in the case of real-valued sequential data, is not always easy or even possible to visually evaluate the generated data. For example, the ICU signals with which we work in this paper, could look completely random to a non-medical expert.

Therefore, in this work, we start by demonstrating our model with a number of toy datasets that can be visually evaluated. Next, we use a set of quantifiable methods that can be used as an indicator of the data quality.

3.1.1 Maximum Mean Discrepancy

We consider a GAN successful if it implicitly learns the distribution of the true data. We assess this by studying the samples it generates. This is the ideal setting for maximum mean discrepancy (MMD) [10], and has been used as a training objective for generative moment matching networks [17]. MMD asks if two sets of samples - one from the GAN, and one from the true data distribution, for example - were generated by the same distribution. It does this by comparing *statistics* of the samples. In practice, we consider the squared difference of the statistics between the two sets of samples (the MMD^2), and replace inner products between (functions of) the two samples by a kernel. Given a kernel $K : X \times Y \rightarrow \mathbb{R}$, and samples $\{x_i\}_{i=1}^N, \{y_j\}_{j=1}^M$, an unbiased estimate of MMD^2 is:

$$\widehat{MMD}_u^2 = \frac{1}{n(n-1)} \sum_{i=1}^n \sum_{j \neq i}^n K(x_i, x_j) - \frac{2}{mn} \sum_{i=1}^n \sum_{j=1}^m K(x_i, y_j) + \frac{1}{m(m-1)} \sum_{i=1}^m \sum_{j \neq i}^m K(y_i, y_j)$$

Defining appropriate kernels between time series is an area of active research. However, much of the challenge arises from the need to align time series. In our case, the generated and real samples are already aligned by our fixing of the ‘time’ axis. We opt then to treat our time series as vectors (or matrices, in the multidimensional case) for comparisons, and use the radial basis function (RBF) kernel using the squared ℓ_2 -norm or Frobenius norm between vectors/matrices; $K(x, y) = \exp(-\|x - y\|^2/(2\sigma^2))$. To select an appropriate kernel bandwidth σ we maximise the estimator of the t-statistic of the power of the MMD test between two distributions [24]; $\hat{t} = \frac{\widehat{MMD}^2}{\sqrt{V}}$,

where V is the asymptotic variance of the estimator of MMD^2 . We do this using a split of the validation set during training - the rest of the set is used to calculate the MMD^2 using the optimised bandwidth. Following [24], we define a mixed kernel as a sum of RBF kernels with two different σ s, which we optimise simultaneously. We find the MMD^2 to be more informative than either generator or discriminator loss, and correlates well with quality as assessed by visualising.

3.1.2 Train on Synthetic, Test on Real (TSTR)

We propose a novel method for evaluating the output of a GAN when a supervised task can be defined on the domain of the training data. We call it “Train on Synthetic, Test on Real” (TSTR). Simply put, we use a dataset generated by the GAN to train a model, which is then tested on a held-out set of true examples. This requires the generated data to have labels - we can either provide these to a conditional GAN, or use a standard GAN to generate them in addition to the data features. In this work we opted for the former, as we describe below. For using GANs to share synthetic ‘de-identified’ data, this evaluation metric is the gold standard, because it demonstrates the ability of the synthetic data to be used for real applications. We present the pseudocode for this GAN evaluation strategy in Algorithm 1.

Algorithm 1 Train on Real, Test on Synthetic

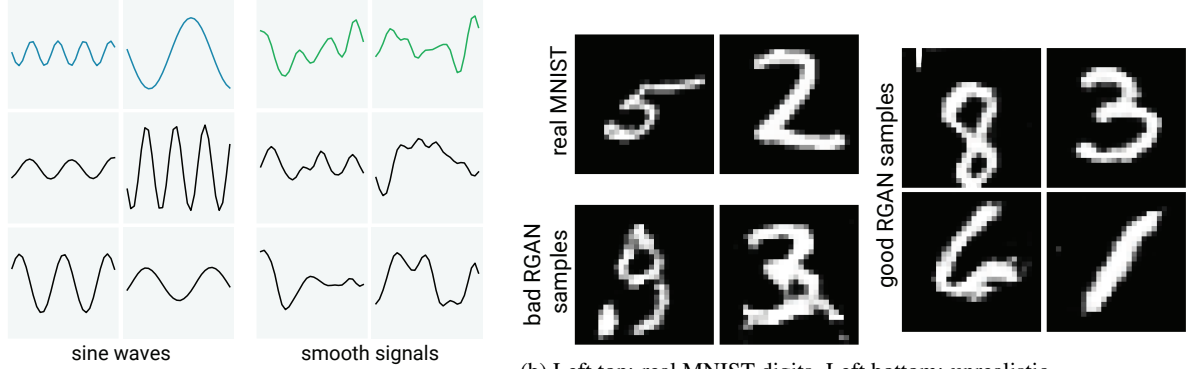
```

1: train, test = split(data)
2: discriminator, generator = train_GAN(train)
3: with labels from train:
4:   synthetic = generator.generate_synthetic(labels)
5:   classifier = train_classifier(synthetic, labels)
6:   If validation set available, optionally optimise GAN over classifier performance.
7: with labels and features from test:
8:   predictions = classifier.predict(features)
9:   TSTR_score = score(predictions, labels)

```

3.1.3 Train on Real, Test on Synthetic (TRTS)

Similar to the TSTR method proposed above, we consider the reverse case, called “Train on Real, Test on Synthetic” (TRTS). In this approach, we use real data to train a supervised model on a set of tasks. Then, we generate a synthetic dataset with a RCGAN, and we evaluate the model’s performance on that set, using the *generated* labels as ground truth. If the supervised model trained with real data assigns to the synthetic data the same labels than had been assigned to it by the GAN, then it is a strong indication that such synthetic data contains realistic features.



(a) Examples of real (coloured, top) and generated (black, lower two lines) samples.

(b) Left top: real MNIST digits. Left bottom: unrealistic digits generated at epoch 27. Right: digits with minimal distortion generated at epoch 100.

Figure 2: RGAN is capable of generating realistic-looking examples.

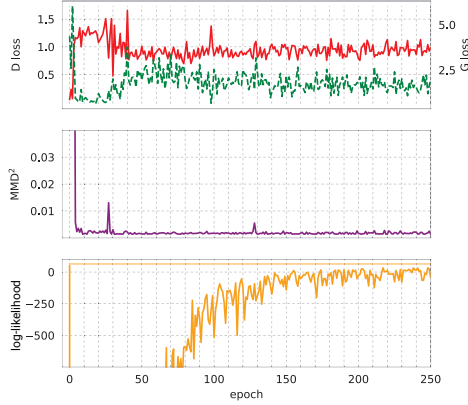


Figure 3: Trace of generator (dotted), discriminator (solid) loss, MMD^2 score and log likelihood of generated samples under the data distribution during training for RGAN generating smooth sequences (output in Figure 2a.)

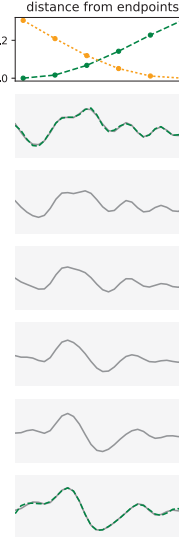


Figure 4: Back-projecting training examples into the latent space and linearly interpolating them produces smooth variation in the sample space. Top plot shows sample-space distance from top (green, dashed) sample to bottom (orange, dotted). Distance measure is RBF kernel with bandwidth chosen as median pairwise distance between training samples. The original training examples are shown in dotted lines in the bottom and second-from-top plots.

4 Learning to generate realistic sequences

To demonstrate the model’s ability to generate ‘realistic-looking’ sequences in controlled environments, we consider several experiments on synthetic data. In the experiments that follow, unless otherwise specified, the synthetic data consists of sequences of length 30. We focus on the non-conditional model RGAN in this section.

4.1 Sine waves

The quality of generated sine waves are easily confirmed by visual inspection, but by varying the amplitudes and frequencies of the real data, we can create a dataset with nonlinear variations. We generate waves with frequencies in $[1.0, 5.0]$, amplitudes in $[0.1, 0.9]$, and random phases between $[-\pi, \pi]$. The left of Figure 2a shows examples of these signals, both real and generated (although they are hard to distinguish).

We found that, despite the absence of constraints to enforce semantics in the latent space (as in [6]), we could alter the frequency and phase of generated samples by varying the latent dimensions,

	Accuracy
Real	0.997 ± 0.00008
TRTS	0.976 ± 0.0013
TSTR	0.951 ± 0.0007

Table 1: Scores obtained by a Convolutional Neural Network when: a) trained and tested on real data, b) trained on real and tested on synthetic, and c) trained on synthetic and tested on real data.

although the representation was not ‘disentangled’, and one dimension of the latent space influenced multiple aspects of the signal.

4.2 Smooth functions

Sine waves are simple signals, easily reproduced by the model. In our ultimate medical application, we wish the model to reproduce complex physiological signals which may not follow simple dynamics. We therefore consider the harder task of learning arbitrary smooth signals. Gaussian processes offer a method to sample values of such smooth functions. We use a RBF kernel with to specify a GP with zero-valued mean function. We then draw 30 equally-spaced samples. This amounts to a single draw from a multivariate normal distribution with covariance function given by the RBF kernel evaluated on a grid of equally-spaced points. In doing so, we have specified exactly the probability distribution generated the true data, which enables us to evaluate generated samples under this distribution. The right of Figure 2a shows examples (real and generated) of this experiment. The main feature of the real and generated time series is that they exhibit smoothness with local correlations, and this is rapidly captured by the RGAN.

Because we have access to the data distribution, in Figure 3 we show how the average (log) likelihood of a set of *generated* samples increases under the data distribution during training. This is an imperfect measure, as it is blind to the *diversity* of the generated samples - the oft-observed mode collapse, or ‘Helvetica Scenario’ [9] of GANs - hence we prefer the MMD² measure. It is nonetheless encouraging to observe that, although the GAN objective is unaware of the underlying data distribution, the likelihood of the generated samples improve with training.

4.3 MNIST as a Time Series

The MNIST hand-written digit dataset is ubiquitous in machine learning research. Accuracy on MNIST digit classification is high enough to consider the problem ‘solved’, and generating MNIST digits seems an almost trivial task for traditional GANs. However, we are unaware of any attempts to generate MNIST digits using a recurrent architecture. Taking inspiration from the serialisation of MNIST in the long-memory RNN literature [14], where each 28×28 digit forms a 784-dimensional vector, we convert MNIST into a *sequence* and aim to generate it with the RGAN. The benefit of using MNIST this way, is that we can use it to train our RGAN and RCGAN models, and then easily visualize the generated sequences as one image, in order to assess its quality.

To make the task more tractable and to explore the RGAN’s ability to generate *multivariate* sequences, we treat each 28x28 image as a sequence of 28, 28-dimensional outputs. We show two types of experiment with this dataset. In the first one, we train a RGAN to generate MNIST digits in this sequential manner. Figure 2b demonstrates how realistic the generated digits appear.

For the second experiment, we downsample the MNSIT digits to 14x14 pixels, and consider the first three digits (0, 1, and 2). With this data we train a RCGAN and subsequently perform the TRTS and TSTR evaluations explained above, for the task of classifying the digits. That is, for the TSTR evaluation, we use real data to train an MNIST classifier, and then we check if the labels assigned by this classifier to the synthetic data, are the same that were provided to the GAN to generate it. For the TRTS evaluation, we train an MNIST classifier with the data generated by our RCGAN data, and then evaluate the performance of this classifier on the task of evaluating real MNIST digits. Results of this experiment are show in Table 1. To obtain error bars on the accuracies reported, we trained the RCGAN five times with different random initialisations. As we can see, the RCGAN manages to generate a purely synthetic dataset which is realistic enough to train a classifier which achieves high performance on real data.

5 Learning to generate realistic ICU data

One of the main goals of this paper is to build a model capable of generating realistic medical datasets, and specifically ICU data. For this purpose, we based our work on the recently-released Philips eICU database¹. This dataset was collected by the critical care telehealth program provided by Philips. It contains around 200,000 patients from 208 care units across the US, with a total of 224,026,866 entries divided in 33 tables.

From this data, we focus on generating the four most frequently recorded, regularly-sampled variables measured by bedside monitors: oxygen saturation measured by pulse oximeter (SpO₂), heart rate (HR), respiratory rate (RR) and mean arterial pressure (MAP). In the eICU dataset, these variables are measured every five minutes. To reduce the length of the sequences we consider, we downsample to one measurement every fifteen minutes, taking the median value in each window. This greatly speeds up the training of our LSTM-based GAN while still capturing the relevant dynamics of the data.

In the following experiments, we consider the *beginning* of the patient’s stay in the ICU, considering this a critical time in their care. We focus on the first 4 hours of their stay, which results in 16 measurements of each variable. While medical data is typically fraught with missing values, in this work we circumvented the issue by discarding patients with missing data (after downsampling). After preprocessing the data this way, we end up with a cohort of 17,693 patients. Most restrictive was the requirement for non-missing MAP values, as these measurements are taken invasively.

5.1 TSTR tasks in eICU

The data generated in a ICU is complex, so it is challenging for non medical experts to spot patterns or trends on it. Thus, one plot showing synthetic ICU data would not provide enough information to evaluate its actual similarity to the real data. Therefore, we evaluate the performance of the ICU RCGAN using the TSTR method.

To perform the TSTR evaluation, we need a supervised task (or tasks) on the data. A relevant question in the ICU is whether or not a patient will become ‘critical’ in the near future - a kind of early warning system. For a model generating dynamic time-series data, this is especially appropriate, as *trends* in the data are likely most predictive. Based on our four variables (SpO₂, HR, RR, MAP) we define ‘critical thresholds’ and generate binary labels of whether or not that variable will exceed the threshold in the next hour of the patient’s stay - that is, between hour 4 and 5, since we consider the first four hours ‘observed’. The thresholds are shown in the columns of Table 2. There is no upper threshold for SpO₂, as it is a percentage with 100% denoting ideal conditions.

As for MNIST, we ‘sample’ labels by drawing them from the real data labels, and use these as conditioning inputs for the RCGAN. This ensures the label distribution in the synthetic dataset and the real dataset is the same, respecting the fact that the labels are not independent (a patient is unlikely to simultaneously suffer from high and low blood pressure), while not leaking personal health information.

Following Algorithm 1, we train the RCGAN for 1000 epochs, saving one version of the dataset every 50 epochs. Afterwards, we evaluate the synthetic data using TSTR. We use cross validation to select the best synthetic dataset based on the classifier performance, but since we assume that it might be also used for unknown tasks, we use only 3 of the 7 tasks of interest to perform this cross validation step (denoted in italics in Table 2). The results of this experiment are presented in Table 2, which compares the performance achieved by a random forest classifier that has been trained to predict the 7 tasks of interest, in one experiment with real data and in a different experiment with the synthetically generated data.

6 Is the GAN just memorising the training data?

One explanation for the TSTR performance in MNIST and eICU could be that the GAN is simply “memorising” the training data and reproducing it. If this were the case, then the (potentially private) data used to train the GAN would be leaked, raising privacy concerns when used on sensitive medical

¹<https://eicu-crd.mit.edu/>

		<i>SpO₂ < 95</i>	<i>HR < 70</i>	<i>HR > 100</i>
AUROC	real	0.9587 ± 0.0004	0.9908 ± 0.0005	0.9919 ± 0.0002
	TSTR	0.88 ± 0.01	0.96 ± 0.01	0.95 ± 0.01
	random	0.5	0.5	0.5
AUPRC	real	0.9059 ± 0.0005	0.9855 ± 0.0002	0.9778 ± 0.0002
	TSTR	0.66 ± 0.02	0.90 ± 0.02	0.84 ± 0.03
	random	0.16	0.26	0.18
		<i>RR < 13</i>	<i>RR > 20</i>	<i>MAP < 70</i>
AUROC	real	0.9735 ± 0.0001	0.963 ± 0.001	0.9717 ± 0.0001
	TSTR	0.86 ± 0.01	0.84 ± 0.02	0.875 ± 0.007
	random	0.5	0.5	0.5
AUPRC	real	0.9557 ± 0.0002	0.891 ± 0.001	0.9653 ± 0.0001
	TSTR	0.73 ± 0.02	0.50 ± 0.06	0.82 ± 0.02
	random	0.26	0.1	0.39
			<i>MAP > 110</i>	
AUROC	real			0.960 ± 0.001
	TSTR			0.87 ± 0.04
	random			0.5
AUPRC	real			0.8629 ± 0.0007
	TSTR			0.42 ± 0.07
	random			0.05

Table 2: Performance of random forest classifier for eICU tasks when trained with real data and when trained with synthetic data (test set is real), including random prediction baselines. AUPRC stands for area under the precision-recall curve, and AUROC stands for area under ROC curve. Italics denotes those tasks whose performance were optimised in cross-validation.

data. It is key that the training data for the model should not be recoverable by an adversary. In addition, while the typical GAN objective incentivises the generator to reproduce training examples, we hope that it does not overfit to the training data, and learn an implicit distribution which is peaked at training examples, and negligible elsewhere.

To answer this question we perform three tests - one qualitative, two statistical, outlined in the next subsections:

6.1 Comparing the distribution of reconstruction errors

To test if the generated samples look "too similar" to the training set, we could generate a large number of samples and calculate the distance to the nearest neighbour (in the training set) to each generated sample. We could compare the distribution of these distances with those comparing the generated samples and a held-out test set. However, to get an accurate estimate of the distances, we may need to generate many samples, and correspondingly calculate many pairwise distances. Instead, we *intentionally generate* the nearest neighbour to each training (or test) set point, and then compare the distances.

We generate these nearest neighbours by minimising the reconstruction error between target y and the generated point; $\mathcal{L}_{\text{recon}}(y)(Z) = 1 - K(G(Z), y)$ where K is the RBF kernel described in 3.1.1, with bandwidth σ chosen using the median heuristic [5]. We find Z by minimising the error until approximate convergence (when the gradient norm drops below a threshold).

We can then ask if we can distinguish the *distribution* of reconstruction errors for different input data. Specifically, we ask if we can distinguish the distribution of errors between the training set and the test set. The intuition is that if the model has "memorised" training data, it will achieve identifiably lower reconstruction errors than with the test set. We use the Kolmogorov-Smirnov two-sample test to test if these distributions differ. For the RGAN generating sine waves, the p-value is 0.2 ± 0.1 , for smooth signals it is 0.09 ± 0.04 , and for the MNIST experiment shown in Figure 2b it is 0.38 ± 0.06 . We conclude that the model has not memorised the training data.

6.2 Interpolation

Suppose that the model has overfit, and most points in latent space map to training examples. If we take a smooth path in the latent space, we expect that at each point, the corresponding generated sample will have the appearance of the "closest" (in latent space) training example, with little variation until we reach the attractor basin of another training example, at which point the samples switch appearance.

We test this qualitatively as follows: we sample a pair of training examples (we confirm by eye that they don't look "too similar"), and then "back-project" them into the latent space to find the closest corresponding latent point, as described above. We then linearly interpolate between those latent points, and evaluate the generator at each point. Figure 4 shows an example of this procedure using the "smooth function" dataset. The samples show a clear incremental variation between start and input sequences, contrary to what we would expect if the model had simply memorised the data.

6.3 Comparing the generated samples

Rather than using a nearest-neighbours approach, we can use the MMD three-sample test [5] to compare the full set of generated samples. With X being the generated samples, Y and Z being the training and test set respectively, we ask if the MMD between X and Y is less than the MMD between X and Z . We performed this test for the generated eICU data used in section 5.1 and found a p-value of 0.40 ± 0.05 that the training data has a smaller MMD with the generated samples than the test data does, which was not sufficient for us to reject the null hypothesis that these MMD scores are significantly different. Similarly, for the MNIST data in section 4.3, the p-value is 0.53 ± 0.09 . For the sine waves, smooth signals and higher-resolution MNIST RGAN experiments in section 4, the p-values were 0.41 ± 0.07 , 0.07 ± 0.04 , and 0.59 ± 0.12 respectively.

7 Conclusion

We have described, trained and evaluated a recurrent GAN architecture for generating real-valued sequential data, which we call RGAN. We have additionally developed a conditional variant (RCGAN) to generate synthetic *datasets*, consisting of real-valued time-series data with associated labels. As this task poses new challenges, we have presented novel solutions to deal with evaluation and questions of privacy. By generating labelled training data - by conditioning on the labels and generating the corresponding samples, we can evaluate the quality of the model using the 'TSTR technique', where we train a model on the synthetic data, and evaluate it on a real, held-out test set. We have demonstrated this approach using 'serialised' multivariate MNIST, and on a dataset of real ICU patients, where models trained on the synthetic dataset achieved performance at times comparable to that of the real data. In domains such as medicine, where privacy concerns hinder the sharing of data, this implies that with refinement of these techniques, models could be developed on *synthetic* data that are still valuable for real tasks. This could enable the development of synthetic 'benchmarking' datasets for medicine (or other sensitive domains), of the kind which have enabled great progress in other areas. We have additionally illustrated that such a synthetic dataset does not pose a major privacy concern or constitute a data leak for the original sensitive training data.

References

- [1] Martín Abadi, Ashish Agarwal, Paul Barham, Eugene Brevdo, Zhifeng Chen, Craig Citro, Greg S. Corrado, Andy Davis, Jeffrey Dean, Matthieu Devin, Sanjay Ghemawat, Ian Goodfellow, Andrew Harp, Geoffrey Irving, Michael Isard, Yangqing Jia, Rafal Jozefowicz, Lukasz Kaiser, Manjunath Kudlur, Josh Levenberg, Dan Mané, Rajat Monga, Sherry Moore, Derek Murray, Chris Olah, Mike Schuster, Jonathon Shlens, Benoit Steiner, Ilya Sutskever, Kunal Talwar, Paul Tucker, Vincent Vanhoucke, Vijay Vasudevan, Fernanda Viégas, Oriol Vinyals, Pete Warden, Martin Wattenberg, Martin Wicke, Yuan Yu, and Xiaoqiang Zheng. TensorFlow: Large-scale machine learning on heterogeneous systems, 2015. Software available from tensorflow.org.
- [2] Grigory Antipov, Moez Baccouche, and Jean-Luc Dugelay. Face aging with conditional generative adversarial networks. *arXiv preprint arXiv:1702.01983*, 2017.
- [3] Martin Arjovsky, Soumith Chintala, and Léon Bottou. Wasserstein GAN. 26 January 2017.
- [4] Martin Arjovsky, Amar Shah, and Yoshua Bengio. Unitary evolution recurrent neural networks. In *International Conference on Machine Learning*, pages 1120–1128, 2016.
- [5] Wacha Boulniphone, Eugene Belilovsky, Matthew B Blaschko, Ioannis Antonoglou, and Arthur Gretton. A test of relative similarity for model selection in generative models. 14 November 2015.

- [6] Xi Chen, Yan Duan, Rein Houthooft, John Schulman, Ilya Sutskever, and Pieter Abbeel. InfoGAN: Interpretable representation learning by information maximizing generative adversarial nets. 12 June 2016.
- [7] Edward Choi, Siddharth Biswal, Bradley Malin, Jon Duke, Walter F Stewart, and Jimeng Sun. Generating multi-label discrete electronic health records using generative adversarial networks. 19 March 2017.
- [8] Jon Gauthier. Conditional generative adversarial nets for convolutional face generation. *Class Project for Stanford CS231N: Convolutional Neural Networks for Visual Recognition, Winter semester, 2014*(5):2, 2014.
- [9] Ian J Goodfellow, Jean Pouget-Abadie, Mehdi Mirza, Bing Xu, David Warde-Farley, Sherjil Ozair, Aaron Courville, and Yoshua Bengio. Generative adversarial networks. 10 June 2014.
- [10] Arthur Gretton, Karsten M Borgwardt, Malte Rasch, Bernhard Schölkopf, and Alex J Smola. A kernel method for the two-sample-problem. In *Advances in neural information processing systems*, pages 513–520, 2007.
- [11] Ishaan Gulrajani, Faruk Ahmed, Martin Arjovsky, Vincent Dumoulin, and Aaron Courville. Improved training of wasserstein GANs. 31 March 2017.
- [12] Sepp Hochreiter and Jürgen Schmidhuber. Long short-term memory. *Neural computation*, 9(8):1735–1780, 1997.
- [13] Stephanie L Hyland and Gunnar Rätsch. Learning unitary operators with help from $u(n)$. In *AAAI 2017*, 2017.
- [14] Quoc V Le, Navdeep Jaitly, and Geoffrey E Hinton. A simple way to initialize recurrent networks of rectified linear units. *arXiv preprint arXiv:1504.00941*, 2015.
- [15] Christian Ledig, Lucas Theis, Ferenc Huszár, Jose Caballero, Andrew Cunningham, Alejandro Acosta, Andrew Aitken, Alykhan Tejani, Johannes Totz, Zehan Wang, et al. Photo-realistic single image super-resolution using a generative adversarial network. *arXiv preprint arXiv:1609.04802*, 2016.
- [16] Jiwei Li, Will Monroe, Tianlin Shi, Alan Ritter, and Dan Jurafsky. Adversarial learning for neural dialogue generation. *arXiv preprint arXiv:1701.06547*, 2017.
- [17] Yujia Li, Kevin Swersky, and Richard Zemel. Generative moment matching networks. 10 February 2015.
- [18] Mehdi Mirza and Simon Osindero. Conditional generative adversarial nets. *arXiv preprint arXiv:1411.1784*, 2014.
- [19] Olof Mogren. C-RNN-GAN: Continuous recurrent neural networks with adversarial training. 29 November 2016.
- [20] F. Pedregosa, G. Varoquaux, A. Gramfort, V. Michel, B. Thirion, O. Grisel, M. Blondel, P. Prettenhofer, R. Weiss, V. Dubourg, J. Vanderplas, A. Passos, D. Cournapeau, M. Brucher, M. Perrot, and E. Duchesnay. Scikit-learn: Machine learning in Python. *Journal of Machine Learning Research*, 12:2825–2830, 2011.
- [21] Alec Radford, Luke Metz, and Soumith Chintala. Unsupervised representation learning with deep convolutional generative adversarial networks. *arXiv preprint arXiv:1511.06434*, 2015.
- [22] Scott Reed, Zeynep Akata, Xinchen Yan, Lajanugen Logeswaran, Bernt Schiele, and Honglak Lee. Generative adversarial text to image synthesis. In *Proceedings of The 33rd International Conference on Machine Learning*, volume 3, 2016.
- [23] Tim Salimans, Ian Goodfellow, Wojciech Zaremba, Vicki Cheung, Alec Radford, and Xi Chen. Improved techniques for training GANs. 10 June 2016.
- [24] Dougal J Sutherland, Hsiao-Yu Tung, Heiko Strathmann, Soumyajit De, Aaditya Ramdas, Alex Smola, and Arthur Gretton. Generative models and model criticism via optimized maximum mean discrepancy. 14 November 2016.
- [25] Lucas Theis, Aäron van den Oord, and Matthias Bethge. A note on the evaluation of generative models. 5 November 2015.
- [26] Yuhuai Wu, Yuri Burda, Ruslan Salakhutdinov, and Roger Grosse. On the quantitative analysis of Decoder-Based generative models. 14 November 2016.

- [27] Zhen Yang, Wei Chen, Feng Wang, and Bo Xu. Improving neural machine translation with conditional sequence generative adversarial nets. *arXiv preprint arXiv:1703.04887*, 2017.
- [28] Lantao Yu, Weinan Zhang, Jun Wang, and Yong Yu. SeqGAN: Sequence generative adversarial nets with policy gradient. 18 September 2016.